A UV Survey of B Supergiants: Continuum Properties

D. Massa

Hughes STX, NASA/GSFC, Greenbelt, MD 20771, USA

R. K. Prinja

Dept. of Physics & Astronomy, University College London, Gower Street, London WC1E 6BT, UK

Abstract. We report our ongoing investigation into the photospheric properties of B supergiants. We review the spectroscopic diagnostics which make the B supergiants ideal for several types of studies, and then discuss initial progress made in determining their intrinsic flux distributions. We also include a discussion of LTE model parameters and our plans for producing a uniform high-dispersion data base.

1. Introduction

Considerable work has been done on the UV properties of the atmospheres and winds of O stars (e.g., Howarth & Prinja 1989, Massa & Savage 1985, Lamers & Leitherer 1993, Puls et al. 1996), but relatively little on normal B supergiants (BIs hereafter). This is a serious oversight, since the UV spectra of BIs contain a rich assortment of wind and photospheric lines from a wide range of ionizations, making them ideal for studying the physics of hot-star winds and atmospheres.

Some specific properties of BI spectra include:

(*i*) The photospheric UV silicon lines in BIs are sensitive temperature and luminosity diagnostics (see Massa 1989; Walborn, Parker & Nichols 1995).

(*ii*) The strongest UV photospheric lines in BIs are affected by velocity gradients in their upper atmospheres/lower winds (Massa, Shore & Wynne 1992; Lamers & Achmad 1994). Consequently, these lines are potential diagnostics of this poorly understood region of stellar-wind flows. Figure 1 (adapted from Massa et al. 1992) demonstrates this effect for luminous B1 stars. The spectra are aligned on the relatively weak C II λ1324Å line. As one moves to more luminous types, the components of the strong Si III $\lambda\lambda$1300 multiplet become progressively more asymmetric, and shifted by about -50 km s^{-1} relative to the less luminous stars. Furthermore, Massa et al. show that even the C II line is affected.

(*iii*) The wind lines in BIs respond to abundance differences (Walborn & Panek 1984) and can be used to determine quantitative relative abundances (Massa et al. 1991), providing important information on the evolutionary history of these stars. Although limited, this approach has the advantage of bypassing the complications involved with analyzing 'photospheric' lines formed in an in-

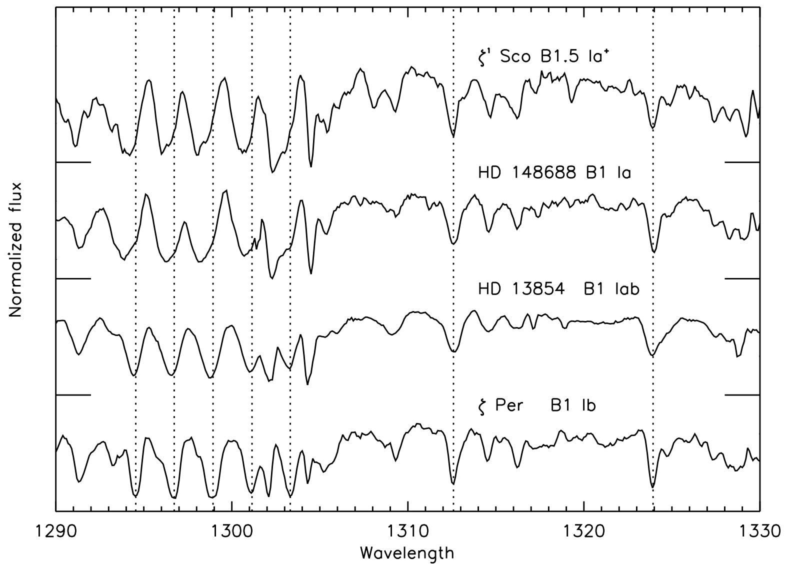

Figure 1. Progression of velocity gradients in luminous B stars.

trinsically dynamic atmosphere. Figure 2 compares selected spectral regions of the BN1 Ib star HD 93840 and the normal B1 Ib ζ Per. Notice that although these stars have similar photospheric spectra and Si IV wind-line profiles, the N V $\lambda\lambda1240$ doublet in HD 93840 is far stronger than in ζ Per, while its C IV $\lambda\lambda1550$ doublet is much weaker. This peculiar behavior was shown to result from a strong nitrogen overabundance (Walborn et al. 1990) and was analyzed by Massa et al. to derive quantitative relative abundances for the two stars.

(*iv*) The wind lines in BIs are often well-developed, but unsaturated. This has two important consequences. First, it enables one to derive well-determined ionic abundances for the wind lines, sometimes including ions from consecutive stages of ionization (see Prinja & Massa 1998). Secondly, this property makes the wind lines extremely sensitive diagnostics of stellar-wind variability (Massa, Prinja & Fullerton 1995). Figure 3 is from Massa et al. (1995) and shows how dramatic wind variability can be in normal B supergiants.

For these reasons, it is important to have well-determined, quantitative measurements of BI photospheric and wind line strengths to provide the basic material needed to derive empirical relationships among the observables, and to test the theoretical models needed to extract intrinsic stellar information.

We are currently analyzing high- and low-dispersion IUE spectra of a sample of 113 normal BIs. Prinja & Massa (1998) discuss the initial results on the wind lines, while this paper discusses the progress made on the photospheric analysis.

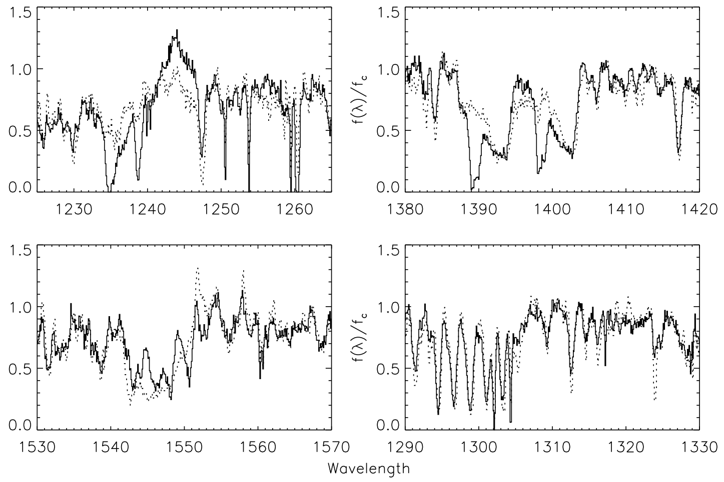

Figure 2. The effects of abundance anomalies on the wind lines of intermediate-luminosity BIs. Full line, ζ Per; dotted line, HD 93840.

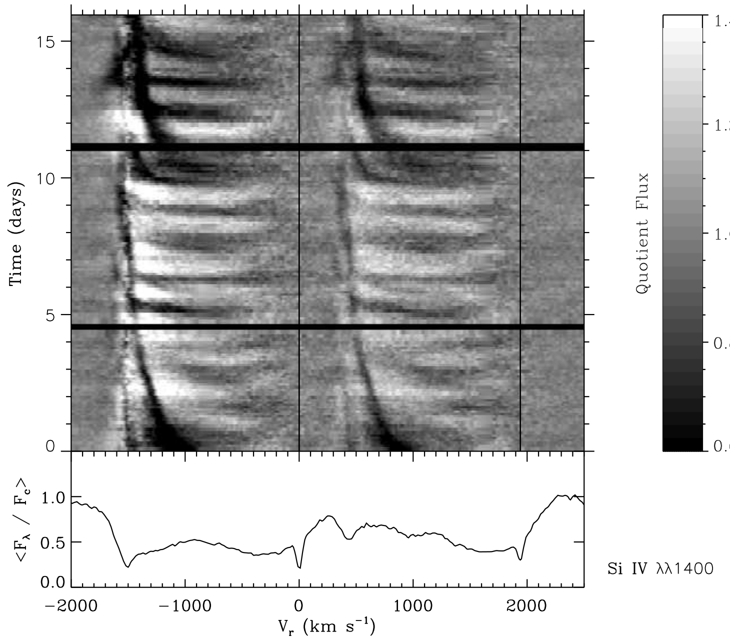

Figure 3. Dynamic spectrum of highly systematic wind variability in the B0.5 Ib star HD 64760; see Prinja et al. (1995) and Fullerton et al. (1997) for further details.

2. The Photospheres of B Supergiants

We have begun our investigation of the photospheres of B supergiants by determining their UV energy distributions from IUE low-dispersion spectra. Our long-range goals include quantitative measurements of high-dispersion spectra, but determining the intrinsic flux distributions turns out to be an integral part of this process, as we discuss below.

Unreddened UV continua of BIs have the following applications:

(*i*) Since they are sensitive only to ensembles of lines, they provide a robust means of testing models and of inferring stellar parameters, without a detailed understanding of the formation of individual lines.

(*ii*) Since they often represent the best data available for faint (distant) objects, or when dealing with large numbers of objects, a grid of intrinsic continua for well-studied stars is needed to place such information into context.

(*iii*) Since many BIs have no true UV continuum, the low-dispersion continua will provide a guide for making quantitative line measurements and rigorous comparisons to models. The situation is especially complicated for unshepherded high-dispersion spectra of rapidly rotating BIs.

(*iv*) Since they are intrinsically bright, BIs have been the preferred targets for studying extinction in other galaxies. This application requires a grid of unreddened standard stars for comparison to the extragalactic, reddened stars.

Table 1: The Continuum Grid

	Ia	Iab	Ib	II	III
B0	ϵ Ori NGC 3293		69 Cyg		HD 63922 NGC 4755
B0.5	κ Ori HD 167756 NGC 3293		HD 64760	NGC 3293	NGC 3293
B1		ρ Leo	HD 86606 γ Ara HD 214080 h & χ Per NGC 3293	HD 215733 h & χ Per NGC 3293	h & χ Per NGC 3293 NGC 4755
B2	h & χ Per		HD 165024 h & χ Per	h & χ Per	HD 51283 h & χ Per NGC 4755
B3	o^2 CMa h & χ Per NGC 4755				HD 79447
B5	η CMa		ϕ Vel 67 Oph	HD 83183	o Cas HD 209419
B8	β Ori h & χ Per		HD 46769		27 Tau
B9	NGC 4755	σ Cyg			20 Pav

Previous work has been done on the continua of luminous B stars. For example, Cardelli et al. (1992) considered a very limited sample for the purpose of extinction studies. Also, Fanelli et al. (1992) developed a coarse grid for use in spectral-synthesis models. Consequently, they only derived a few 'representative' types and ignored some of the complications we will address in detail.

Assembling a complete grid of intrinsic UV continua for BIs is difficult. The reason is that there are very few unreddened BIs, and the shapes of UV reddening curves vary from one line of sight to another (see, e.g., Fitzpatrick & Massa 1986). To overcome these problems, we adopt the approach employed by Massa & Savage (1985) to determine O-star continua. We consider only lightly reddened stars – $E(B-V) \leq 0.15$ – or stars which are members of clusters. In the former case, the errors introduced by a variable extinction curve are minimal (Massa 1987), and in the latter case the extinction toward a cluster can be derived from its main-sequence B stars and analyzed to determine whether its shape is uniform across the cluster (Massa & Fitzpatrick 1986).

The clusters containing B supergiants used to supplement the lightly reddened grid are: $h\,\&\,\chi$ Per, NGC 3293, NGC 4755, and NGC 6231. Table 1 lists the stars in our grid. Between the two groups, we have excellent spectral coverage and adequate redundancy to verify our results.

3. Initial Results

3.1. Morphological Properties

Figures 4–6 display examples of our results to date. Figure 4 shows how UV continua respond to luminosity class for a fixed spectral type of B5 (all the spectra are normalized to V). The continua become progressively 'flatter' in the UV at higher luminosity. This reflects the effects of a decrease in both $T_{\rm eff}$ and surface gravity in the higher luminosity-class stars.

Figure 5 shows an extreme case of how luminosity affects the UV continuum. It compares the UV continuum of the B1.5 hypergiant ζ^1 Sco (thick line, dereddened by an extinction curve applicable to Sco OB1) to those of a B2 Ib and a B3 Ia. Notice that, while the continuum of the hypergiant agrees with that of a B2 Ib in the near UV, it more closely approximates that of a B3 Ia in the far UV.

Figure 6 compares the dereddened fluxes of lightly reddened stars with similar cluster stars, dereddened by extinction curves determined from the main-sequence cluster members (Massa & Fitzpatrick 1986). For the two cluster stars shown, the agreement is excellent.

3.2. Comparison to Models

This is very much work in progress. Our initial modelling consists of comparing selected BIs to Kurucz models. Although the physics in these models is certainly inadequate for many luminous B stars, they are capable of fitting the detailed spectral features. We fit the low-dispersion IUE spectra normalized to their V flux. We used the transformation to the HST absolute-flux scale determined by Fitzpatrick & Massa (in prep.). For the lightly reddened stars, a Cardelli et al. (1988) $R = 3.1$ curve was used to correct the UV flux, and $E(B-V)$ was deter-

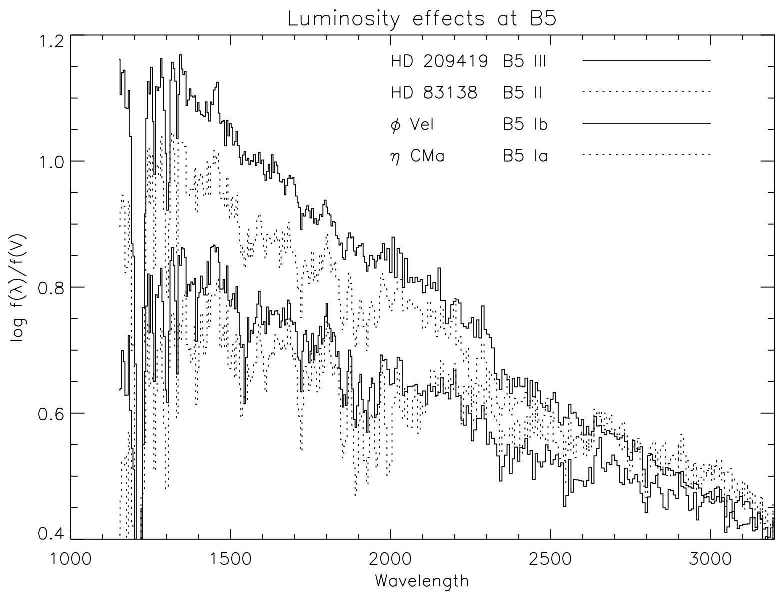

Figure 4. Effects of luminosity on the UV continua of B5 stars. The more luminous stars have 'flatter' far-UV continua, and stronger lines.

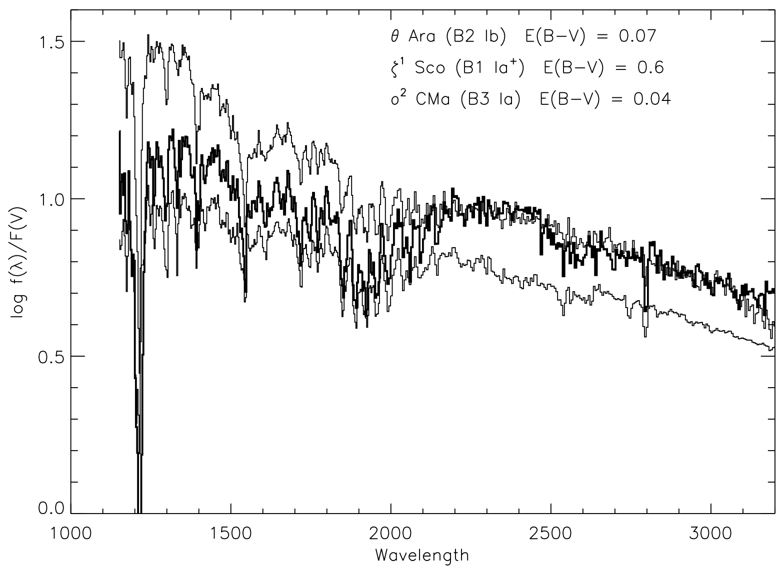

Figure 5. An extreme example of how luminosity can affect the UV continuum of a luminous B star. The thick curve is the continuum of the hypergiant ζ^1 Sco.

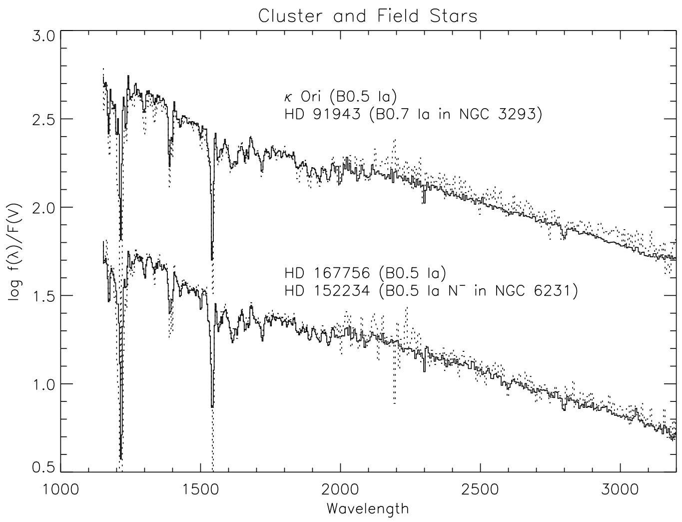

Figure 6. Comparison of dereddened spectra of lightly reddened stars (solid curves) and cluster stars dereddened using extinction curves derived from the cluster main-sequence B stars (dotted curves). The quality of the cluster spectra is poor in the region of the 2175Å extinction bump, where the uncorrected flux is low.

mined consistently with the model fit. Examples of the fits are shown in Figs. 7 and 8. Finally, the atmospheric parameters were combined with the Schaller et al. (1992) interior models to obtain physical parameters for the programme stars. We see that, for mid- and early-B stars of intermediate luminosity, the physical parameters determined by the fits are sensible. On the other hand, for the cooler and more luminous stars, even though the models can still produce a good fit to the observations, the implied physical parameters are clearly incorrect.

4. Future Directions

The unreddened continua discussed above will be used for two purposes. The first is part of a larger project meant to determine the region of the HR diagram where hydrostatic, LTE, line-blanketed models provide an accurate, physically meaningful description of the observations (Fitzpatrick & Massa, in prep.).

The second is to produce unreddened *high-dispersion* spectra for all of our 113 programme stars. This is a *multi-step* process, beginning with a grid of unreddened SWP spectra rebinned to low dispersion. Then, for each programme star we:

1. determine the χ^2 of a fit of the programme star to a linear combination of *each* grid star and the three SWP reddening functions (the FUV curvature term, a component which is linear in λ^{-1}, and the strength of a standard 2175Å bump),

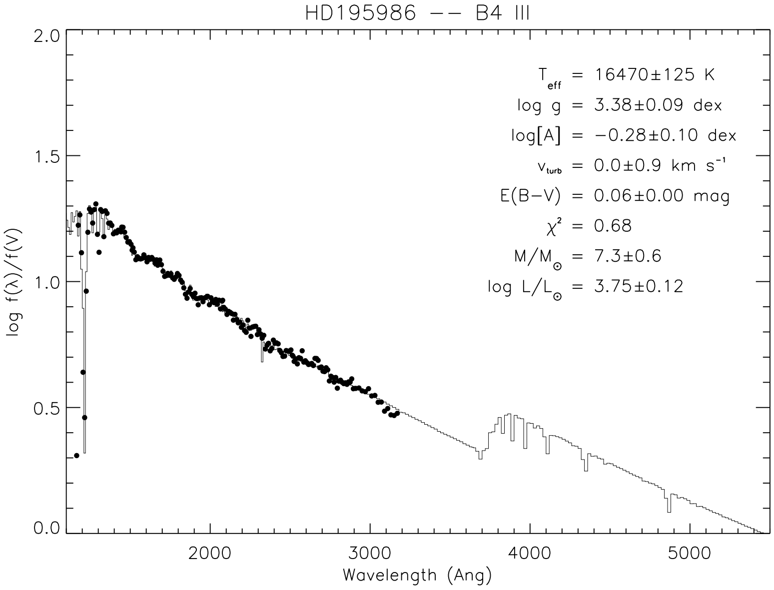

Figure 7. Model fit to HD 195986. Notice that the best-fitting microturbulent velocity is zero, and that the derived mass and luminosity are reasonable.

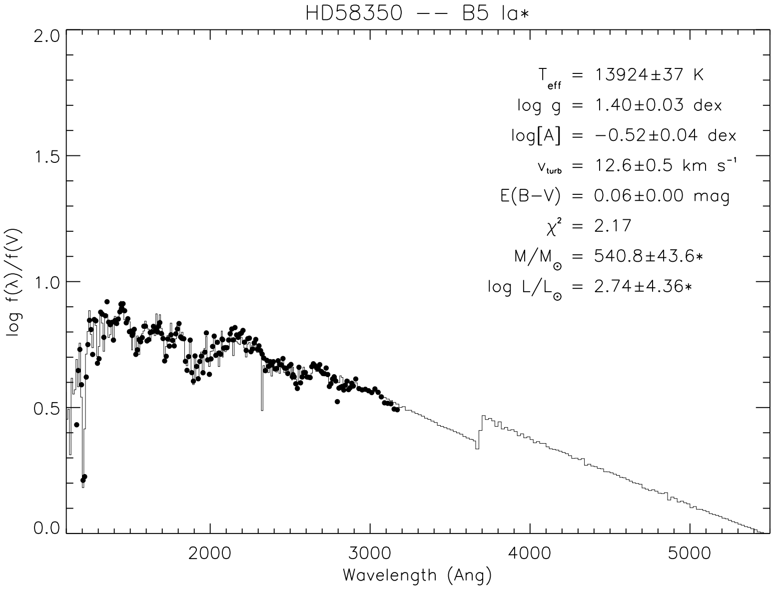

Figure 8. Model fit to η CMa. Although the model does an excellent job of fitting the details of the spectrum, the implied physical parameters are clearly incorrect, being extrapolations of the model grid.

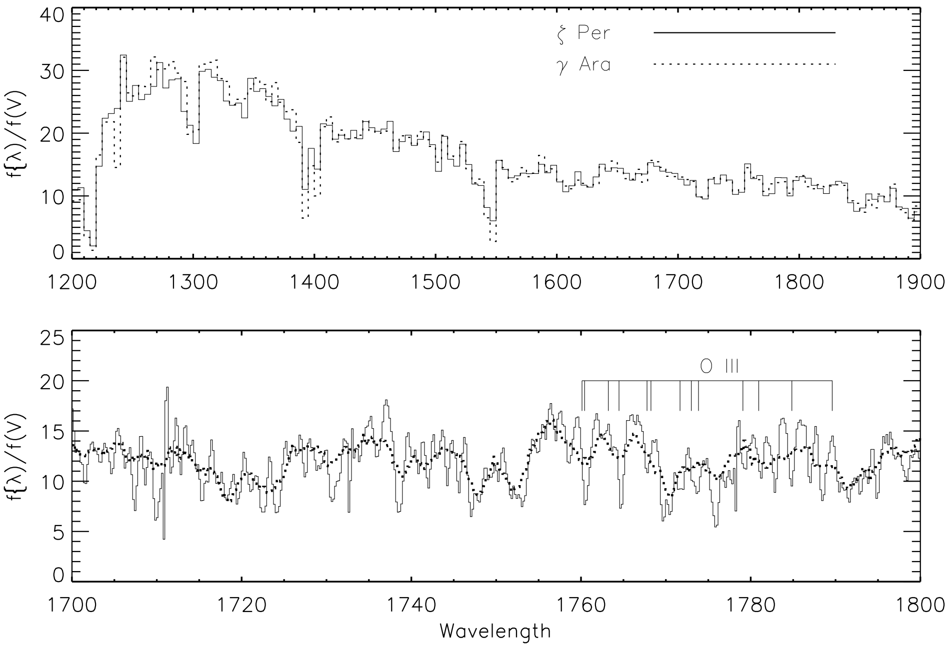

Figure 9. Comparison of dereddened low- and high-dispersion spectra of two B1 Ib stars: ζ Per (solid) and γ Ara (dotted). The upper panel shows their spectra binned to 5-Å resolution, and the lower panel shows a section of the spectra, including several strong O III lines, at 0.2-Å resolution.

2. determine the location of the minimum χ^2 on the grid, and interpolate to determine the best reddening coefficients, and

3. apply these coefficients to deredden the programme star.

The result is an unreddened high-dispersion spectrum for each star which can be used for empirical measurements and to compare with models. Furthermore, the continuum placement is quantifiable, depending only upon the coefficients of the reddening functions.

The process has been tested and is currently progressing. It involves several technical details concerning the time-degradation corrections for IUE high-dispersion spectra and absolute calibrations. Figure 9 shows an example of the results. It compares the spectra of the rapidly rotating B1 Ib star γ Ara and a normally rotating B1 Ib, ζ Per. By applying the reddening functions, their low-resolution spectra can be made to agree very well. Once they are adjusted to a common scale, their high-resolution properties can be examined on an equal footing. These are compared in the lower panel. It is clear that without the low-dispersion spectrum to set the scale, one could be led to very different continuum placements for quantitative measurements, including the strengths of the important, strong O III lines in the region.

Acknowledgments. We gratefully acknowledge partial support by NATO and by NASA contract S-57790-Z. We would also like to thank Ed Fitzpatrick for allowing us to use results prior to publication.

References

Cardelli, J. A, Clayton, G. C., Mathis, J. S., 1988, ApJ, 329, L33

Cardelli, J. A., Sembach, K. R., Mathis, J. S., 1992, AJ, 104, 1916

Fannelli, M. N., O'Connell, R. W., Burstein, D., Wu, C.-C., 1992, ApJS, 82, 197

Fitzpatrick, E. L., Massa, D., 1990, ApJS, 72, 163

Fullerton, A. W., Massa, D. Prinja, R. K., Owocki, S. P., Cranmer, S. R., 1997, A&A, in press

Howarth, I. D., Prinja, R. K., 1989, ApJS, 69, 527

Lamers, H. J. G. L. M., Achmad, L., 1994, A&A, 291, 856

Lamers, H. J. G. L. M., Leitherer, C., 1993, ApJ, 412, 771

Massa, D., 1987, AJ, 94, 1675

Massa, D., 1989, A&A, 224, 131

Massa, D., Altner, B., Wynne, D., Lamers, H. J. G. L. M., 1991, A&A, 242, 188

Massa, D., Fitzpatrick, E. L., 1986, ApJS, 60, 305

Massa, D., Prinja, R. K., Fullerton, A. W., 1995, ApJ, 452, 842

Massa, D., Savage, B. D., 1985, ApJ, 299, 905

Massa, D., Shore, S. N. Wynne, D., 1992, A&A, 264, 169

Prinja, R. K., Massa, D., 1998, in Boulder-Munich II: Properties of Hot, Luminous Stars (ASP Conf. Series, Vol. 131), ed. I. D. Howarth (ASP, San Francisco), p. 218

Prinja, R. K., Massa, D., Fullerton, A. W., 1995, ApJ, 452, L61

Puls, J., et al., 1996, A&A, 305, 171

Schaller, D., Schaerer, D., Meynet, G., Maeder, A., 1992, A&AS, 96, 269

Walborn, N. R., Fitzpatrick, E. L., Nichols-Bohlin, J., 1990, PASP, 102, 543

Walborn, N. R., Panek, R. J., 1984, ApJ, 280, L27

Walborn, N. R., Parker, J. W., Nichols, J. S., 1995, International Ultraviolet Explorer Atlas of B-Type Spectra from 1200 to 1900Å (NASA RP-1363)

Discussion

Drew: You mentioned the use of HIPPARCOS data for some of your programme stars; there is a problem with parallaxes, the so-called Lutz-Kelker corrections, which is well known in the astrometry community but less so outside. Put crudely, just ignore any results worse than 5σ – with HIPPARCOS, most things beyond 150 pc, which probably means most of your stars.

Kudritzki: However, I was very happy to hear you report that κ Ori is half the distance of ϵ Ori. If you put them at the same distance, then they should have more or less the same luminosity, but ϵ Ori has Hα emission and κ Ori has Hα absorption, and κ Ori just did not fit the wind-momentum–luminosity relationship. For me, now, the problem is solved!